agriculture

MDPI

Article

Scenario-Based Modeling of Agricultural Nitrous Oxide Emissions in China

Miaoling Bu [1], Weiming Xi [1], Yu Wang [2] and Guofeng Wang [3,*]

[1] Law School, Shanxi University of Finance and Economics, 140 Wucheng Road, Xiaodian District, Taiyuan 030006, China; buml@stu.sxufe.edu.cn (M.B.); vipxwm@163.com (W.X.)
[2] Business School, Beijing Technology and Business University, Beijing 100048, China; wangyu2021@btbu.edu.cn
[3] Institute of Platform Economics, Shanxi University of Finance and Economics, Taiyuan 030006, China
* Correspondence: wanggf@sxufe.edu.cn; Tel.: +86-180-0126-8337

Abstract: Agricultural land in China represents a major source of nitrous oxide (N_2O) emissions, and as population growth and technological advancements drive agricultural intensification, these emissions are projected to increase. A thorough understanding of historical trends and future dynamics of these emissions is critical for formulating effective mitigation strategies and advancing progress toward the Sustainable Development Goals. This study quantifies N_2O emissions across 31 provinces in China from 2000 to 2021, employing the IPCC coefficient method alongside China's provincial greenhouse gas inventory guidelines. The spatiotemporal evolution of emission intensities was examined, with the Stochastic Impacts by Regression on Population, Affluence, and Technology (STIRPAT) model employed to assess the influence of population, technological development, economic growth, and energy structure. The findings confirm that agricultural land remains the primary source of N_2O emissions, with significantly higher levels observed in eastern coastal regions compared to western inland areas. Implementing targeted mitigation strategies, such as enhanced agricultural- and manure-management practices and region-specific interventions, is imperative to effectively curb the rising emission trends.

Keywords: nitrous oxide from agricultural sources; IPCC coefficient method; spatiotemporal evolution; scenario forecasting

Citation: Bu, M.; Xi, W.; Wang, Y.; Wang, G. Scenario-Based Modeling of Agricultural Nitrous Oxide Emissions in China. *Agriculture* **2024**, *14*, 2074. https://doi.org/10.3390/agriculture14112074

Academic Editor: Efstratios Loizou

Received: 12 October 2024
Revised: 11 November 2024
Accepted: 14 November 2024
Published: 18 November 2024

1. Introduction

Effectively managing non-CO_2 greenhouse gas emissions (non-CO_2 GHG emissions) from agricultural activities is crucial for China to fulfill its climate commitments [1]. Among these emissions, nitrous oxide (N_2O) from agricultural activities stands out as a key contributor due to its high global warming potential and significant role in the agricultural emissions profile [2–4]. N_2O, the third largest greenhouse gas after carbon dioxide (CO_2) and methane (CH_4), has a global warming potential 265 times that of CO_2 and depletes the ozone layer [5]. N_2O has a 114-year atmospheric lifetime [6] and has steadily risen in concentration since 1750 [7], reaching 332 ppb in 2021. N_2O emissions in agriculture are primarily driven by nitrogen fertilizer use, significantly increasing anthropogenic emissions. Overall, global per capita fertilizer use rose from 3 kg in 1960 to 15 kg in 2018 [8]. Over the past decade, global soil N_2O emissions have increased by 59% from pre-industrial levels, with agricultural soils contributing 82% [9]. In China, agricultural N_2O emissions surged from 889.6 Gg/year in 1980 to 2295.0 Gg/year in 2020 [10]. Despite the 2024 government report's emphasis on emissions reduction and climate governance, national policies still prioritize CO_2, lacking regulation for non-CO_2 greenhouse gases, which may hinder broader mitigation efforts [11]. Given that agricultural N_2O emissions are a critical driver of climate change [12], accurately assessing current emissions and future trends in this sector is essential for achieving China's "carbon peaking" and "carbon neutrality" goals. Studies

indicate that the carbon emission intensity in cities of the Yangtze River Delta exhibits significant spatial clustering closely linked to the agricultural scale, crop structure, and resource use efficiency [13].

Prior research has systematically evaluated various techniques to mitigate non-CO_2 GHG emissions from agricultural activities, demonstrating that approaches such as emission accounting, targeted reduction strategies, and scenario-based simulations provide structured frameworks for effective emission control and sustainability advancements in the agricultural sector [14,15]. Techniques targeting agricultural N_2O emissions are crucial given N_2O's significant role in agricultural greenhouse gas profiles [16]. The IPCC's method for greenhouse gas inventories, adaptable across regions, is widely adopted internationally.

In comparison, methodologies like Life Cycle Assessment (LCA) [17,18], meta-analysis [19,20], and Computable General Equilibrium (CGE) models [21,22] are less frequently utilized. Moreover, major international organizations and databases, including the World Bank (WB), the World Resources Institute (WRI), and the Emissions Database for Global Atmospheric Research (EDGAR), have also adopted the IPCC emission factor method to compile inventories of non-CO_2 GHG emissions from agricultural sources [23,24]. Limiting global warming to 1.5 °C requires substantial reductions in agricultural CH_4 and N_2O emissions, which account for approximately 10–12% of total anthropogenic greenhouse gases [25]. For the 1.5 °C target, a 22% reduction in N_2O emissions is required from 2020 to 2050 [26]. Studies suggest that, without cutting non-CO_2 emissions, achieving net-zero CO_2 may need to be accelerated by around 20 years, making integrated mitigation strategies essential [27].

In China, cost-effective mitigation scenarios project that by 2030, reductions in CH_4, fluorinated gases, and N_2O could reach 35%, 30%, and 40%, respectively, from 2015 levels. Measures such as straw incorporation [28], converting cropland to forests or grasslands [29], and promoting energy crops [30] have proven effective in offsetting agricultural greenhouse gas emissions, including N_2O. Integrated mitigation strategies are more effective than single approaches in reducing greenhouse gas emissions, especially for addressing the complexities of agricultural N_2O emissions. This study focuses on agricultural N_2O's role in China's greenhouse gas profile, offering targeted insights for mitigation. Applying the IPCC inventory method, this research develops region-specific scenarios, analyzes agricultural N_2O emission trends and drivers from 2000 to 2021, and simulates future emissions to support reduction strategies. These findings aim to inform China's climate commitments by providing data-driven insights to optimize regional mitigation policies and enhance sustainable agricultural practices that align with national and global climate goals.

2. Methodology and Data

Figure 1 illustrates the generation process of N_2O from agricultural sources. The main sources of agricultural N_2O emissions include emissions from agricultural land and emissions from animal manure management. The N_2O emissions from agricultural land arise from both direct and indirect emissions. Direct emissions encompass three aspects: firstly, emissions resulting from chemical fertilizers (nitrogen fertilizers, phosphate fertilizers, potash fertilizers, and compound fertilizers); secondly, manure discharge; and thirdly, the emission of crop residues. Indirect emissions are mainly attributed to two pathways: nitrogen oxides and ammonia from fertilizers applied to soils and livestock and poultry manure, which generate N_2O emissions through the process of nitrogen deposition in the atmosphere; nitrogen in the soil enters the water body via leaching or runoff to form N_2O. This process involves nitrogen-cycle mechanisms, including ammonia volatilization, nitrogen migration, and conversion, which influence indirect N_2O emissions. In animal manure management, N_2O emissions are mainly caused by the storage and treatment of organic matter in manure and emissions from nitrogen conversion during nitrification or denitrification.

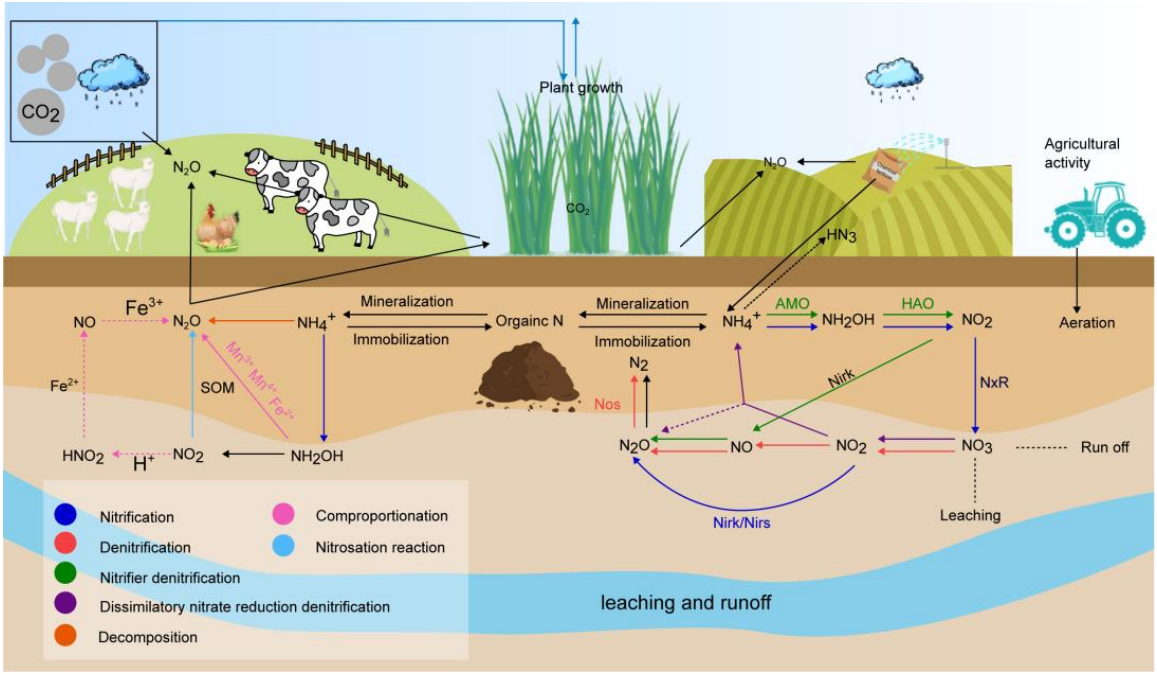

Figure 1. Processes and key drivers of agricultural N_2O production.

2.1. Methodology

In this study, the emission factor methodology of the International Panel on Climate Change (IPCC) was employed to assess the total N_2O emissions from agricultural activities in each provincial administrative region [31]. The selection of the emission factors was conducted in accordance with the 2019 revised edition of the IPCC 2006 Guidelines for the Preparation of Greenhouse Gas Emission Inventories and the relevant data provided in the Guidelines for the Preparation of Provincial Greenhouse Gas Emission Inventories (Trial Version) issued by the National Development and Reform Commission [32]. The IPCC emission factor methodology, suitable for global trend analysis, emphasizes producer responsibility; in contrast, China's provincial guidelines adopt a consumer-focused approach and leverage localized data, enhancing regional specificity and precision—an approach well-suited for nuanced carbon emission management.

$$E_{N_2O} = \sum\left(N_2O_{direct} + N_2O_{deposition} + N_2O_{leaching} + E_{N_2O_{manure}}\right) \quad (1)$$

where E_{N_2O} represents the total volume of N_2O emissions stemming from agricultural sources, N_2O_{direct} represents direct N_2O emissions from crop farmland, $N_2O_{deposition}$ represents indirect emissions of N_2O caused by atmospheric nitrogen deposition, $N_2O_{leaching}$ represents indirect emissions of N_2O from dissolution runoff, and N_2O_{manure} represents the management of N_2O emissions for livestock manure. In this study, the natural breakpoint method was used to classify and analyze the nitrous oxide emissions from agricultural sources in various provinces.

2.2. Accounting Methods for N_2O Emissions from Agricultural Land

In agriculture, N_2O emissions can be divided into two categories: direct and indirect.

2.2.1. Direct Emissions

This source mainly stems from nitrogenous fertilizers applied on agricultural land, such as chemical nitrogen fertilizers and organic fertilizers (manure fertilizer and crop straw). Considering that the application of chemical fertilizers is significantly higher than that of organic fertilizers [33], and data on the use of the latter are often difficult to obtain

accurately, the impact of chemical fertilizers and straw returning is mainly considered when assessing direct N_2O emissions from agricultural land.

$$N_2O_{direct} = \left(N_{fertilizer} + N_{crop\ residue}\right) \times EF_{direct} \quad (2)$$

where N_2O_{direct} represents direct N_2O emissions from agricultural land, $N_{fertilizer}$ indicates the amount of chemical fertilizer applied (nitrogen fertilizer and compound fertilizer), $N_{crop\ residue}$ indicates the nitrogen input of straw returning (aboveground straw returning nitrogen and underground root nitrogen), and EF_{direct} indicates the direct N_2O emission factors from agricultural land (Table 1).

Table 1. Direct emission factors of N_2O from agricultural land (kg N_2O-N per kg of N input).

Region	EF_{direct}	Range
Zone I (Shaanxi, Gansu, Xinjiang, Inner Mongolia, Ningxia, Tibet, Shanxi, Qinghai)	0.0056	0.0015~0.0085
Zone II (Liaoning, Jilin, Heilongjiang)	0.0114	0.0021~0.0258
Zone III (Beijing, Shandong, Hebei, Henan, Tianjin)	0.0057	0.0014~0.0081
Zone IV (Zhejiang, Jiangsu, Shanghai, Chongqing, Hunan, Sichuan, Jiangxi, Hubei, Anhui)	0.0109	0.0026~0.022
Zone V (Hainan, Guangxi, Fujian, Guangdong)	0.0178	0.0046~0.0228
Zone VI (Guizhou, Yunnan)	0.0106	0.0025~0.0218

Note: The data are from the literature [34], and the data from Hong Kong, Macao, and Taiwan are unavailable.

Among them, the equation for calculating nitrogen input from straw returning is shown in Equation (3) [32].

$$N_{crop\ redidue} = \sum_{i=1}^{n}\left[\left(\frac{M_i}{L_i} - M_i\right) \times \beta_i \times K_i + \frac{M_i}{L_i} \times \alpha_i \times K_i\right] \quad (3)$$

where $N_{crop\ residue}$ represents nitrogen used for returning straw, M_i represents the yield of the ith crop in terms of grain, L_i represents the crop's economic coefficient, β_i represents the crop straw return rate, K_i represents the percentage of nitrogen in the crop straw, and α_i represents the root–shoot ratio of crops. The parameters listed in Table 2 follow the standardized values provided in the Guidelines for Provincial Greenhouse Gas Inventory Compilation (Trial) by the National Development and Reform Commission (NDRC).

Table 2. Parameters of the main crops.

Crop Category	Nitrogen Content of the Grain	Nitrogen Content of Straw	Economic Coefficient	Root–Shoot Ratio	Straw Return Rate
Rice	0.01	0.00753	0.489	0.125	0.323
Wheat	0.014	0.00516	0.434	0.166	0.765
Corn	0.017	0.0058	0.438	0.17	0.093
Sorghum	0.017	0.0073	0.393	0.185	0.04
Soybean	0.06	0.0181	0.425	0.13	0.093
Hemp	0.0131	0.0131	0.83	0.25	0.093
Potato	0.004	0.011	0.667	0.05	0.3992
Rapeseed	0.00548	0.00548	0.271	0.15	0.6185
Vegetable leaves	0.008	0.008	0.83	0.25	0.6185
Tobacco	0.041	0.0144	0.83	0.2	0.6185

2.2.2. Indirect Emissions

The equation for calculating N_2O emissions from atmospheric nitrogen deposition is shown in Equation (4) [32].

$$N_2O_{deposition} = \left(N_{livestock} \times 20\% + N_{input} \times 10\%\right) \times 0.01 \quad (4)$$

where $N_{livestock}$ represents the nitrogen content in poultry and livestock manure, and N_{input} represents the nitrogen input of the farmland soil. According to the Guidelines for the Preparation of Provincial Greenhouse Gas Inventories (Trial) for $N_{livestock}$ and N_{input}, the recommended values for nitrogen volatilization rates are 20% and 10%, respectively, and the corresponding emission factors are set at 0.01.

The equation for calculating N_2O emissions caused by leaching runoff is shown in Equation (5) [32].

$$N_2O_{leaching} = N_{input} \times 20\% \times 0.0075 \quad (5)$$

where $N_2O_{leaching}$ indicates the indirect emission of N_2O caused by leaching runoff. The quantity of nitrogen lost by nitrogen leaching and runoff accounted for 20% of the nitrogen input to agricultural land. The N_2O emission factor due to leaching and runoff was 0.0075. Specific parameters can be found in the Guidelines for the Compilation of Provincial Greenhouse Gas Inventories (Trial) issued by the NDRC.

2.3. Accounting Methods for N_2O Emissions from Animal Manure

N_2O emissions from livestock manure management include N_2O from storage and treatment prior to soil application. Equation (6) [32] is as follows:

$$E_{N_2O_{manure}} = \sum_{i=1}^{n} EF_{N_2O_{manure}} \times AP_i \times 10^{-7} \quad (6)$$

Among them, the equation for calculating the nitrogen input from straw return is shown in Equation (3).

where $E_{N_2O_{manure}}$ represents managing N_2O emissions for animal manure, $EF_{N_2O_{manure}}$ represents managing emission factors for livestock and poultry manure in category i, AP_i represents the number of animals in livestock and poultry category i, and the specific parameters are shown in Table 3.

Table 3. Emission factors of greenhouse gases from animal manure management (kg per (head a)).

Region	Dairy Cattle	Non-Dairy Cows	Buffalo	Sheep	Goat	Pig	Poultry	Horse	Donkey/ Mule	Camel
North	1.846	0.794	—	0.093	0.093	0.227				
Northeast	1.096	0.913	—	0.057	0.057	0.266				
East	2.065	0.846	0.875	0.113	0.113	0.175				
Central South	1.710	0.805	0.860	0.106	0.106	0.157				
Southwest	1.884	0.691	1.197	0.064	0.064	0.159				
Northwest	1.447	0.545	—	0.074	0.074	0.195				

Note: The data are sourced from the literature [32].

2.4. Accounting Methods to Determine the Intensity of Non-Carbon Dioxide Greenhouse Gas Emissions from Agricultural Activities

In this study, the intensity of N_2O emissions is assessed by calculating the emissions intensity concerning agricultural value added ($GHGI_1$) and agricultural land area ($GHGI_2$) on a per-unit basis. N_2O emission intensity refers to a metric that measures the amount of nitrous oxide (N_2O) emissions per unit of output. It is calculated as follows:

$$GHGI_{1,J} = \frac{E_j}{G_j} \quad (7)$$

$$GHGI_{2,J} = \frac{E_j}{A_j} \quad (8)$$

where $GHGI_{1,J}$ and $GHGI_{2,J}$ represent the emission intensity per unit of agricultural added value (t CO_2-eq/CNY 10,000) and the emission intensity per unit of agricultural land area (kg CO_2-eq/km^2) of region j, respectively. E_j represents N_2O emissions from agricultural

sources, G_j is the agricultural value added of region j, and A_j is the area of farmland (the arable land plus pasture area) in area j. This study used the natural breakpoint method to classify the N_2O emission intensity of agricultural sources in various provinces of China (including municipalities and autonomous regions).

2.5. N_2O Emission Scenario Prediction Model from Agricultural Activities

This study employs the scalable STIRPAT model to project future nitrous oxide emissions by evaluating the interactions among population, economy, technology, and the environment. The STIRPAT model is fundamentally structured as follows:

$$I = \alpha P^b A^e T^d \varepsilon \tag{9}$$

In the aforementioned equation, I, P, A, and T represent the environmental pressure, demographics, affluence, and technological level. α refers to the constant term of the model, and b, c, and d represent, respectively, the elasticity of the impact of population, income, and technology on environmental pressures. ε represents the model's error term. On this basis, to profoundly analyze the factors affecting N_2O emissions from agricultural activities, the logarithmic processing of both sides of the model was conducted to obtain the following:

$$InI = Ina + bInP + cInA + dInT + eInG + fInAG + gInRP + In\varepsilon \tag{10}$$

where b, c, d, e, f, and g represent the coefficients of each index; P denotes demographics; A represents GDP per capita; T denotes the total power of agricultural machinery, indicating the degree of agricultural mechanization; G represents the effective irrigation area of agriculture, reflecting the status and stability of agricultural production and operation; AG represents the gross agricultural output value, reflecting the scale of rural economic development; and RP represents the size of the rural population and demonstrates the level of urbanization.

To verify the Kuznets curve (EKC) of China's agricultural N_2O environment, this study incorporated the secondary and tertiary terms of the per capita gross domestic product (GDP) into the analysis model to investigate whether there is a "U" or "N"-shaped relationship between per capita GDP and N_2O emissions. The model is presented as follows:

$$InI = Ina + bInP + cInA + m(InA)^2 + n(InA)^3 + dInT + eInG + fInAG + gInRP + In\varepsilon \tag{11}$$

This study employed the methods of literature review, policy document review, and existing data trend analysis to construct three distinct levels of change: low, medium, and high (Table 4). Data from 2000 to 2021 were selected and applied to the STIRPAT model for an in-depth analysis. Based on the unique attributes of different regions, a series of scenarios were developed, and a baseline model was constructed to predict the potential trends in N_2O emissions from agricultural activities in each region from 2025 to 2050. The growth rates in the baseline scenario were set based on government plans and historical trends, while those in the high and low scenarios were adjusted according to the literature to ensure that the analysis captures potential economic and social variations.

Table 4. Rate of change setting.

Variable	Level of	Time Period of Change		
	Change (%)	2025–2030	2031–2040	2041–2050
Demographic [35]	Low	0.5	0.10	1.50
	Middle	1.00	0.60	1.10
	High	1.50	0.20	0.70

Table 4. *Cont.*

Variable	Level of Change (%)	Time Period of Change		
		2025–2030	2031–2040	2041–2050
GDP per capita [36]	Low	2.50	2.0	1.50
	Middle	3.50	3.00	2.50
	High	5.50	4.50	3.50
Agricultural mechanization [37]	Low	3.00	2.50	2.00
	Middle	3.50	3.00	2.50
	High	4.00	3.50	3.00
Effectively irrigated area	Low	0.07	0.10	0.15
	Middle	0.10	0.13	0.18
	High	0.13	0.16	0.21
Agricultural output value [38]	Low	2.90	3.10	3.20
	Middle	3.30	3.50	3.60
	High	3.40	3.60	3.70
Rural populations [35]	Low	−2.00	−1.00	−0.50
	Middle	−3.50	−2.00	−0.50
	High	−5.00	−3.50	−2.00

Note: The data on the effective irrigated area are derived from statistical data fitting.

2.6. Data

The data range from 2000 to 2021 was selected to comprehensively capture trends in agricultural N_2O emissions in China across various policy phases, technological advancements, and climate initiatives. The crop yield data were sourced from various publications, including the China Statistical Yearbook, the China Agricultural Yearbook, the China Animal Husbandry Yearbook, and local statistical yearbooks. Additionally, the areas of cultivated land and pastureland were obtained from the China Rural Statistical Yearbook, the China Land and Resources Yearbook, and the China Environment Yearbook. ArcGIS 10.8, Origin Pro 2024, and Stata MP 17 were used for data analysis and statistical processing.

3. Results and Discussion

3.1. Evolution of Spatiotemporal Patterns of Nitrous Oxide Emissions from Agricultural Sources

Agricultural land is the dominant source of N_2O emissions (Figure 2). In 2021, national N_2O emissions totaled 77.87 Mt CO_2-eq, with agricultural land contributing 55.13 Mt CO_2-eq and animal manure management contributing 22.75 Mt CO_2-eq. Of the agricultural emissions, 89.32% stemmed from chemical fertilizer application, resulting in 49.39 Mt CO_2-eq. In 2007, N_2O emissions from livestock activities sharply declined due to disease control measures, particularly in response to the H5N1 avian influenza outbreak, the implementation of regulatory policies such as the Measures for the Management of National Meat Reserves and the Animal Disease Quarantine Law, and severe flooding in the Huaihe River Basin. These policies not only curbed emissions in the short term but also catalyzed the adoption of more efficient animal-management practices. Similar environmental and health-related disruptions, including widespread flooding in 2017 and 2018 and the outbreak of African swine fever in 2019, further contributed to significant reductions in emissions from livestock by accelerating advancements in biosecurity and animal health monitoring. The temporal variation in N_2O emissions from agricultural activities has been relatively stable; however, regional disparities are more evident. Emissions have decreased in highly urbanized regions such as Beijing, Tianjin, and Shanghai, where agricultural activities comprise a smaller share of land use and technological improvements in precision farming have reduced fertilizer overuse. Conversely, emissions are rising in regions like Inner Mongolia, Jilin, Heilongjiang, Ningxia, and Xinjiang, where agricultural practices are more extensive and nitrogen-use efficiency technologies have been integrated more slowly. Regions like Tibet, Qinghai, and Ningxia, with smaller agricultural land areas and crops with lower

nitrogen demand (e.g., barley, wheat, and potatoes), demonstrate lower fertilizer use and, consequently, lower N_2O emissions. These policy interventions and economic impacts are clearly reflected in the observed N_2O emission trends, highlighting how a combination of regulatory measures, environmental factors, and technological advancements collectively influence emission patterns over time. However, the effectiveness of these policies varies, with urbanized areas more rapidly adopting low-emission technologies compared to regions dependent on traditional agricultural practices.

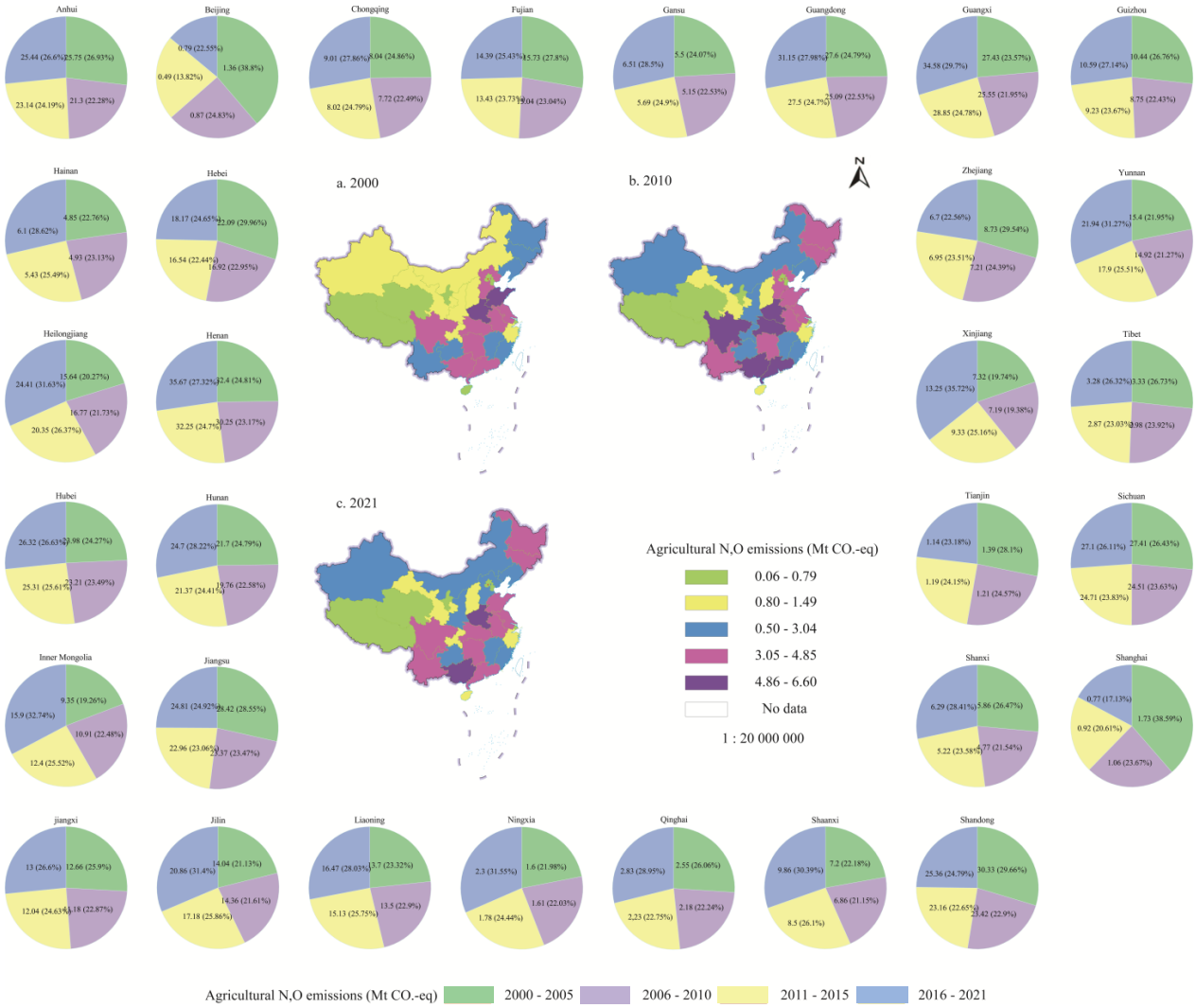

Figure 2. Cumulative agricultural N_2O emissions by province in periods from 2000 to 2021.

From a regional perspective (Figure 3), Eastern, Central, and Southwest China significantly contribute to N_2O emissions in China. Emissions in East China have gradually declined over time, while N_2O emissions in Northeast China have increased year after year, particularly in Heilongjiang. There was no alteration in the proportion of cumulative N_2O emissions in North China and Southwest China during the four time periods, but the specific emissions of each province and region varied. For instance, N_2O emissions in Beijing and Tianjin in Northern China have been decreasing yearly, while in Inner Mongolia, they have been rising.

Figure 3. Cumulative N_2O emissions from agricultural sources by region and period (2000–2021).

In this study, five key time points (2000, 2005, 2010, 2015, and 2021) were selected to analyze the temporal and spatial evolution of N_2O emissions from agricultural sources in China, with a focus on identifying emission types and their provincial distributions.

From a spatiotemporal perspective, total agricultural N_2O emissions exhibited an initial increase, peaking at 69.99 Mt CO_2-eq in 2000 and 84.01 Mt CO_2-eq in 2015, before decreasing to 77.87 Mt CO_2-eq in 2021, reflecting an overall growth of 11.26%. High-emission regions were predominantly located in the southeast of the Yangtze River Basin; southern coastal areas; and provinces such as Henan, Guangdong, Guangxi, Shandong, and Hubei.

Regionally, East China contributed the highest emissions, accounting for 25.33% of the national total, with Jiangsu, Shandong, and Anhui leading within this region. Central China followed, with Henan responsible for 41.20% of the regional emissions, positioning it as the largest emitting province.

Temporal analysis revealed notable increases in emissions from 2000 to 2005 across Central, Northeastern, and Southwestern China, with Inner Mongolia, Xinjiang, Ningxia, Jilin, and Heilongjiang experiencing substantial growth. By 2010, Central and Northeastern China continued to exhibit significant emission increases. In 2015, emissions rose across most regions, with a minor decline observed in Southern China. By 2021, emissions in Northeast China had surged by 47.59% relative to 2000, while East China saw a 15.55% reduction. Although Guangdong, Guangxi, and Henan remained among the highest emitting provinces, their emissions decreased between 2015 and 2021—from 5.66 Mt CO_2-eq to 4.85 Mt CO_2-eq in Guangdong and Guangxi, a reduction of 14.31%, and from 6.6 Mt CO_2-eq to 5.69 Mt CO_2-eq in Henan, a decline of 13.79%.

3.2. Changes in the Emission Intensity of N_2O Gas from Agricultural Sources

The analysis of N_2O emission intensity from agricultural sources is fundamental for informing environmental policy decisions. Figure 4a–c depicts the spatiotemporal distribution of N_2O emissions per unit of agricultural value added. In 2000, provinces such as Zhejiang, Tianjin, Xinjiang, Shaanxi, Beijing, and Gansu exhibited relatively low emission intensities, whereas a general west-to-east increasing trend was observed in other regions. The provinces of Guangxi, Tibet, and Qinghai reported the highest emission intensities, a trend that persisted throughout the period from 2000 to 2021. Despite regional disparities, national emissions intensity has shown an overall annual decline, largely attributed to the intensification of animal husbandry and advances in industrialization. By 2021, Tibet, Jilin, and Qinghai remained among the provinces with the highest emission intensities, although Qinghai experienced a significant reduction of 85.06%, from 31.26 t CO_2-eq/CNY 10,000 to 4.67 t CO_2-eq/CNY 10,000.

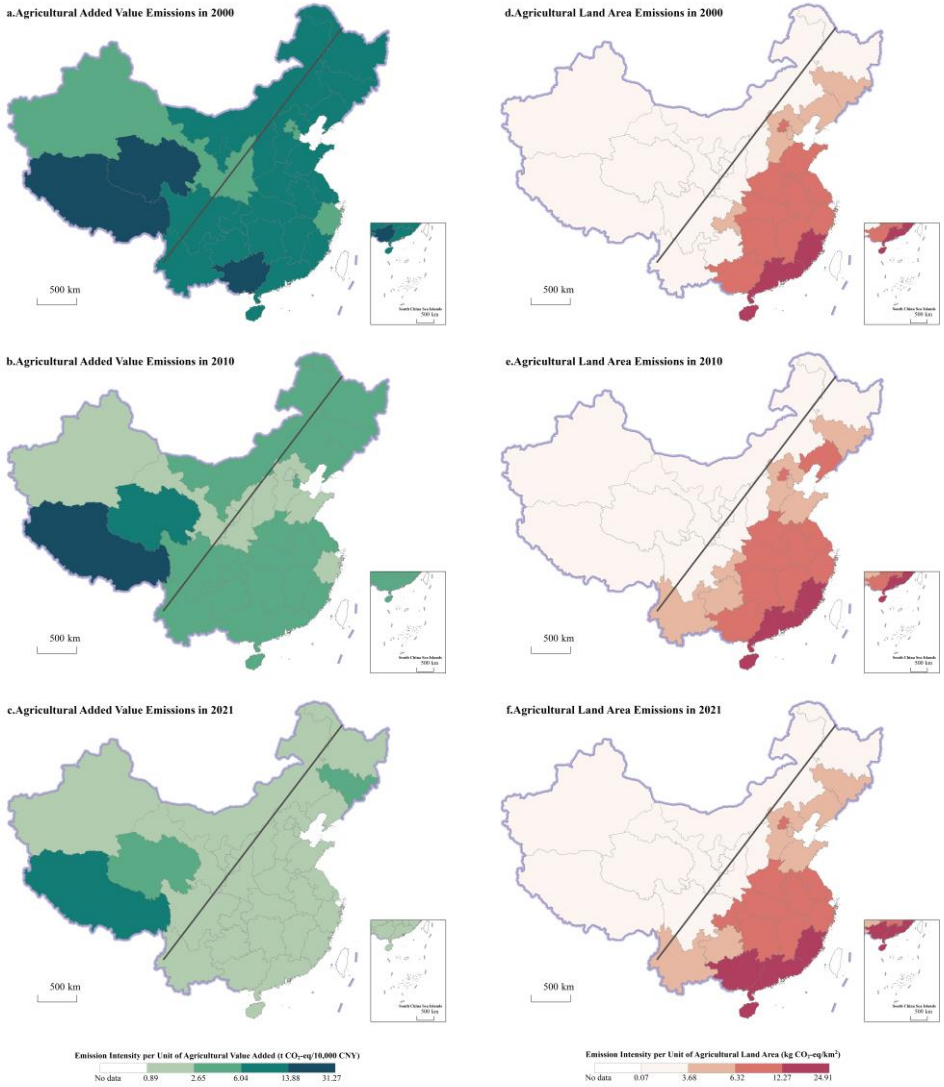

Figure 4. Intensity of agricultural N_2O emissions per unit of agricultural value added and per unit of agricultural land area in 2000, 2010, and 2021.

Figure 4d–f further illustrates the distribution of N_2O emissions per unit of agricultural land area, revealing a clear geographical dichotomy along the "Hu Huanyong Line". The Hu Huanyong Line represents a geographical demarcation in China, frequently used to delineate the spatial distribution of population and economic development. It roughly spans from Heihe in Heilongjiang Province to Tengchong in Yunnan Province. To the west of this line, the population is sparse, and the region is characterized by lower levels of economic development. In contrast, the area to the east is densely populated and exhibits more advanced economic conditions. West of the line, most provinces, except for Beijing, experienced modest increases in emission intensity. In contrast, eastern regions saw more substantial increases, particularly in South China, driven by rapid urbanization and the conversion of agricultural land for construction purposes. Provinces such as Fujian, Hainan, Guangdong, and Guangxi exhibited the highest intensities. In western regions, emission intensity remained below 3.68 kg CO_2-eq/km^2, whereas in eastern regions, values reached up to 24.90 kg CO_2-eq/km^2. This East–West disparity is primarily driven by urbanization processes in the eastern provinces, where the conversion of agricultural land has led to a concentration of emissions relative to the remaining land.

From 2000 to 2021, the N_2O emission intensity per unit of agricultural added value declined across all provinces (Figure 5a). In Jilin Province, the intensity initially decreased

by 5.33 t CO_2-eq/CNY 10,000, followed by a modest increase of 0.46 t CO_2-eq/CNY 10,000. While East China experienced simultaneous reductions in both emissions and agricultural added value intensity, other regions exhibited rising emissions despite declining intensity. For instance, emissions in Northwest China increased by 59.37%, while intensity dropped by 45.70 t CO_2-eq/CNY 10,000. Similarly, emissions in Southwest China rose by 10.68%, with a reduction in intensity of 44.64 t CO_2-eq/CNY 10,000. Tibet exhibited the highest emission intensity nationwide, largely due to its animal husbandry-based agricultural practices and unique geographical and climatic conditions, which result in lower agricultural productivity and higher emission intensity.

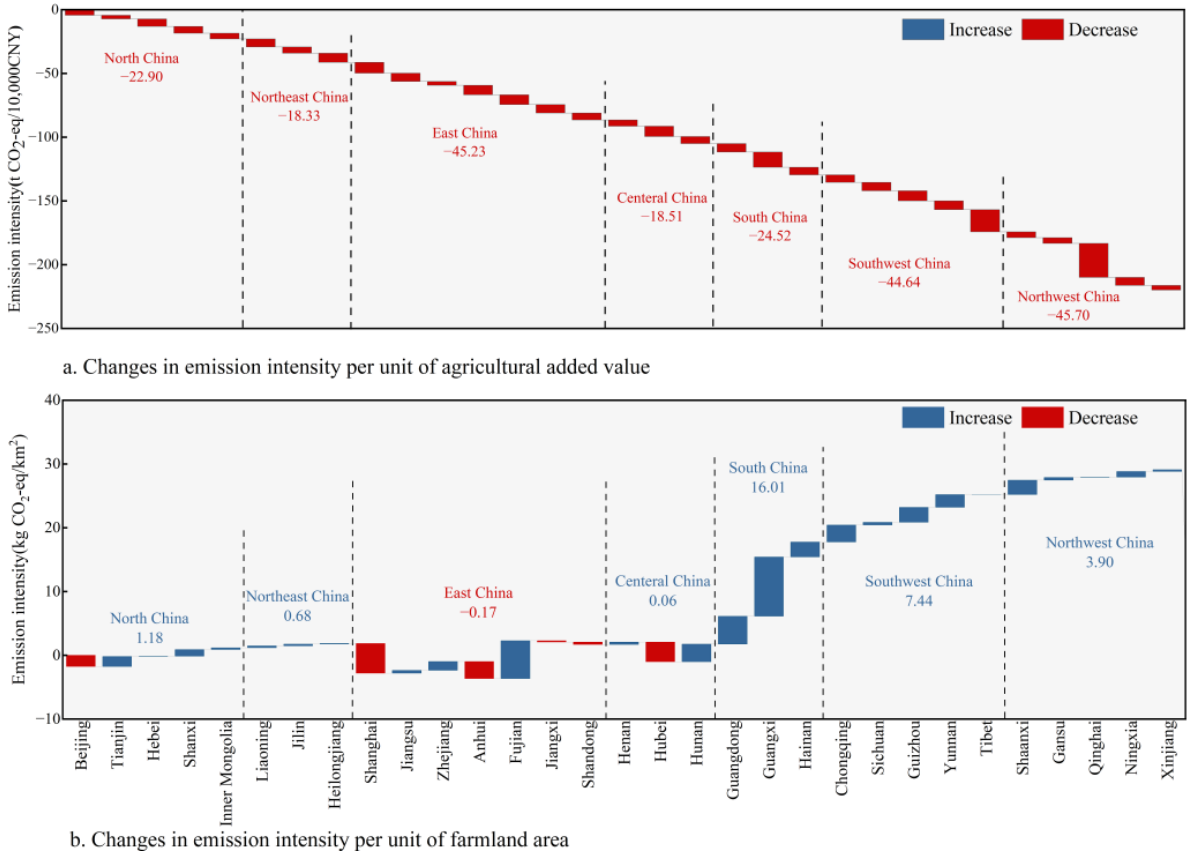

Figure 5. Trends in N_2O emission intensity by province (2000–2021).

Figure 5b illustrates the variation in N_2O emission intensity per unit of agricultural land across provinces. Between 2000 and 2021, Shanghai showed the largest decrease in emission intensity per unit of cultivated land, with a reduction of 4.67 kg CO_2-eq/km^2, reflecting an average annual decline of 1.85%. This trend is mainly attributed to the significant reduction in cultivated land area. Except for East China, all regions demonstrated a general increase in emission intensity per unit of farmland.

3.3. Nitrous Oxide Emission Scenario Projection from Agricultural Sources

This study applied the STIRPAT model to forecast and analyze the peak of N_2O emissions resulting from agricultural activities across 31 provinces in China. Initially, the variables were standardized, followed by a multicollinearity test, which revealed a variance inflation factor (VIF) exceeding 10, indicating significant multicollinearity in the dataset. Additionally, the *p*-values for each region passed the 1% significance threshold based on the Hausman test, which supported the selection of a fixed-effects ridge regression model. In total, 682 observations were included in the analysis, with the regression results of the STIRPAT model presented in Table 5.

Table 5. Regression results of the STIRPAT model.

Argument	InI						
	North	**Northeast**	**East**	**Central**	**South**	**Southwest**	**Northwest**
lnP	0.045	−0.251 ***	−0.037	0.099	0.118 ***	0.112 ***	0.157 ***
	(1.327)	(−6.121)	(−0.434)	(0.898)	(14.522)	(9.655)	(8.487)
lnA	−0.165 ***	0.004	−0.376 ***	−0.071	−0.032 ***	−0.018	0.143 ***
	(−6.914)	(0.385)	(−11.397)	(−2.17)	(−3.627)	(−1.241)	(9.016)
lnT	0.236 ***	0.231 ***	0.065 **	−0.049 **	0.268 ***	0.118 ***	0.011
	(14.105)	(11.735)	(2.421)	(−1.032)	(22.909)	(5.17)	(0.424)
lnG	0.417 ***	0.076 ***	0.367 ***	0.085	0.239 ***	0.389 ***	0.161 ***
	(26.033)	(4.709)	(9.923)	(1.033)	(22.367)	(16.797)	(8.032)
lnAG	0.258 ***	0.06 ***	0.5 ***	0.252 ***	0.058 ***	0.01	0.055 ***
	(16.899)	(4.534)	(13.442)	(6.405)	(4.837)	(0.794)	(5.895)
lnRP	0.083 ***	0.065	0.146 ***	0.195 ***	0.209 ***	0.137 ***	0.2 ***
	(4.963)	(1.644)	(3.45)	(3.064)	(17.6)	(9.118)	(9.515)
Constant terms	−5.917 ***	−0.183	−3.192 ***	−2.468 ***	−5.086 ***	−4.688 ***	−5.296 ***
	(−21.025)	(−0.522)	(−5.857)	(−3.82)	(−52.005)	(−35.53)	(−30.429)
R^2	0.976	0.906	0.935	0.751	0.986	0.95	0.912

Note: The t-statistic is indicated in parentheses; *** and ** are significant at 1% and 5%, respectively.

Population growth in the southern, southwestern, and northwestern regions significantly contributed to N_2O emissions from agricultural sources. However, in Northeast China, while the population increase led to a reduction in emissions, rural population changes had no significant effect. Additionally, increased per capita income was associated with reduced agricultural N_2O emissions in North, East, South, and Northwest China but had no significant impact in other regions.

Agricultural mechanization exacerbated N_2O emissions in North, Northeast, East, South, and Southwest China, while it suppressed emissions in Central China and had no notable effect in Northwest China. The expansion of effective irrigation contributed significantly to N_2O emissions across all regions except Central China, where no substantial impact was detected. Moreover, gross agricultural output consistently intensified N_2O emissions in all regions except Southwest China, where no significant effect was observed.

By incorporating quadratic and cubic terms of per capita GDP into the STIRPAT model, this study confirms the presence of an Environmental Kuznets Curve (EKC) relationship between N_2O emissions and per capita GDP. The regression results (Table 6) indicate that the coefficients of lnA, $(lnA)^2$, and $(lnA)^3$ were $m < 0$, $n > 0$, and $k < 0$, respectively, reflecting an inverted N-shaped relationship. This suggests that N_2O emissions from agricultural activities in China peaked between 2000 and 2021 and are now in decline.

Table 6. EKC curve test of nitrous oxide from agricultural sources.

Argument	InI		
	Model 1	**Model 2**	**Model 3**
lnP	−0.115	−0.002	0.025
	(−1.277)	(−0.026)	(0.28)
lnA	−0.229 ***	−1.262 ***	−3.541 ***
	(−5.557)	(−8.95)	(−4.052)
$(lnA)^2$	-	0.058 ***	0.338 ***
		(7.634)	(3.18)
$(lnA)^3$	-	-	−0.011 ***
			(−2.642)
lnT	−0.027	−0.052	−0.054
	(−0.6)	(−1.218)	(−1.266)
lnG	0.17 ***	0.183 ***	0.177 ***
	(3.894)	(4.383)	(4.239)

Table 6. *Cont.*

Argument	InI		
	Model 1	**Model 2**	**Model 3**
lnAG	0.49 ***	0.521 ***	0.53 ***
	(13.126)	(14.43)	(14.682)
lnRP	0.566 ***	0.52 ***	0.507 ***
	(8.957)	(8.528)	(8.324)
Constant terms	−4.952 ***	−1.105 **	4.847 **
	(−29.189)	(−2.087)	(2.095)
R^2	0.867	0.877	0.878

Note: The t-statistic is indicated in parentheses; *** and ** are significant at 1% and 5%, respectively.

Based on prior research, notable regional disparities in N_2O emissions from agricultural sources are observed across China, with region-specific influencing factors. To account for these differences, this study developed multiple scenarios to model the drivers of N_2O emissions from agricultural activities to predict future emission trends. Scenario forecasting is a method used to predict possible future outcomes by setting different assumptions and conditions. After excluding statistically insignificant variables, we established three scenarios: a baseline scenario (BL), a green development scenario (GD), and an extensive development scenario (ES) for seven regions (Table 7). Using the STIRPAT model, this study projects N_2O emissions from agricultural activities in China from 2025 to 2050 (Figure 6). Furthermore, using the STIRPAT model, this study projects N_2O emissions from agricultural activities across various regions in China from 2025 to 2050.

Table 7. Scenario setting.

Region	North China, Northeast China		East China, Central China		Northwest		South China, Southwest China	
scene	ES	GD	ES	GD	ES	GD	ES	GD
P								
A								
T								
G								
AG								
RP								

Note: GD: green development scenarios, ES: extensive development scenarios. Red: high, Blue: middle, Green: Low.

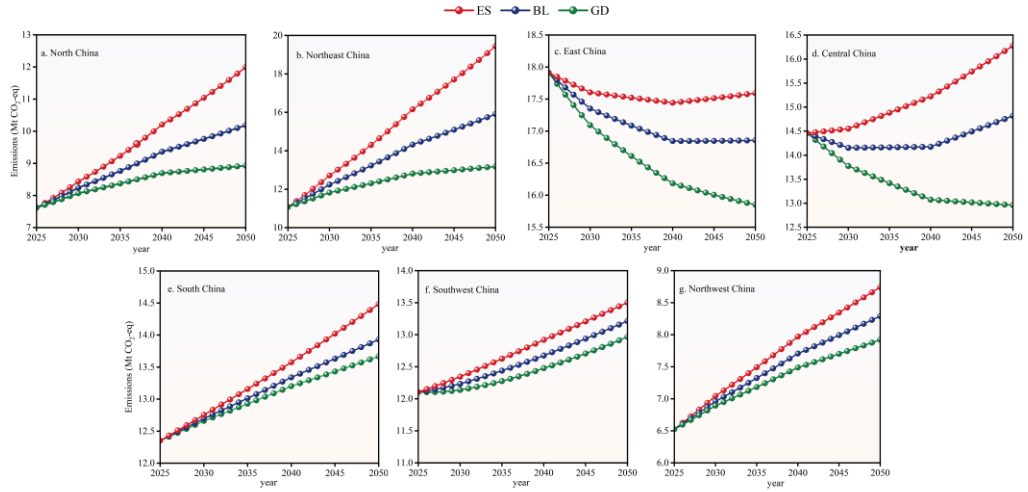

Figure 6. Simulation of regional agricultural N_2O gas emission scenarios.

The prediction results based on the STIRPAT model indicate that, from 2025 to 2050, agricultural N_2O emissions in various regions of China will exhibit the following trends under different development scenarios: green development scenario < baseline scenario < extensive development scenario. In the baseline scenario, agricultural N_2O emissions in the East China region initially decline sharply, but the rate of decrease gradually slows down as influencing factors change, reaching a minimum in 2040 before starting to rise slowly. Emissions in Central China first decrease, then gradually increase, followed by a sharp rise, while emissions in other regions generally increase. In the green development scenario, the growth rate of emissions in North and Northeast China gradually falls below that in South, Southwest, and Northwest China. At the same time, the emissions in East and South China exhibit a downward trend, contrasting with the baseline scenario. Under the extensive development scenario, the emissions in East China first decrease and then increase, but the overall trend remains relatively stable, whereas emissions in other regions rise rapidly. Overall, while the emissions from agricultural activities in East China are expected to continue decreasing, emissions in other regions are projected to increase, posing significant challenges to emission reduction. To achieve effective reductions, it is essential to develop targeted strategies based on the specific characteristics of each region.

Our findings identify manure management and fertilizer application as critical targets for emission reduction in China, particularly considering the high global warming potential of N_2O relative to CO_2, especially from agricultural sources such as fertilizer-applied fields. Effective nitrogen fertilizer management strategies, including precision application [39], nitrogen formulation optimization, crop rotation, and conservation tillage, are essential to minimizing N_2O emissions from agricultural fields [40,41]. Furthermore, drip irrigation has been shown to significantly enhance water and fertilizer efficiency, leading to substantial reductions in N_2O emissions worldwide [42,43]. For manure management, adjusting animal feed to reduce nitrogen content can decrease nitrogen levels in manure, thereby lowering ammonia and N_2O emissions. Composting also helps stabilize organic content, reducing N_2O emissions from manure [44].

China's spatial and temporal diversity in agricultural practices and economic development underscores the need for region-specific mitigation strategies to meet carbon peaking targets by 2030 and achieve carbon neutrality by 2060 [45–47]. This study calculated N_2O emissions in China from 2000 to 2021, identified spatial and temporal trends, and projected future emission scenarios. The selection of emission factors and variability in regional data may introduce certain biases, potentially affecting the precision of emission estimates across regions. Additionally, challenges in collecting comprehensive data on indirect emissions from agricultural sources may lead to underestimations of total emissions.

The limitations of this study, such as variations in emission factors and potential underreporting of indirect emissions, highlight the need for future research to focus on refining emission source classifications and enhancing regional emission factors for greater accuracy. Exploring the impact of manure management on N_2O emissions and developing more advanced predictive models would be beneficial for further progress in this field. Future studies could explore region-specific mitigation strategies tailored to local agricultural practices and environmental conditions. Moreover, considering the future impacts of climate change on agricultural emissions is crucial for ensuring the long-term effectiveness of mitigation efforts.

These findings not only inform China's policies on agricultural emissions reduction but also provide valuable insights for global strategies on sustainable agriculture and climate action.

4. Conclusions

This study employed official statistical data and IPCC-recommended methodologies to calculate N_2O emissions from crop cultivation and manure management across various countries and regions. Using this approach, we analyzed spatial and temporal variations in emission intensities relative to the agricultural value added and land area. Utilizing

the STIRPAT model, we examined the impacts of population, economic, and technological factors on agricultural N_2O emissions, delivering a comprehensive, region-specific analysis. Additionally, we projected future emission trends and explored the Environmental Kuznets Curve (EKC) for N_2O emissions in China, providing critical insights for formulating effective N_2O-mitigation policies.

Our results reveal that farmland is the principal source of agricultural N_2O emissions in China, with chemical fertilizer application as the dominant contributor, especially in Guangxi, Henan, and Shandong. The Ministry of Agriculture's "Zero Growth Action Plans for Fertilizer and Pesticide Use by 2020" has shown effectiveness, with agricultural N_2O emissions peaking around 2015, followed by a steady decline across all regions. Nevertheless, notable regional disparities persist. By 2021, regions east of the Hu Line demonstrated higher emission intensities per unit of cultivated land. In contrast, western regions, particularly agro-pastoral zones, showed higher emissions per unit of agricultural economic output. These patterns reflect variations in resource-use efficiency and environmental costs across China.

These findings highlight the critical role of region-specific policies in advancing China's 2030 carbon-peak and 2060 carbon-neutrality goals. Given the substantial variation in agricultural practices and emission profiles across provinces, implementing tailored mitigation strategies that reflect local conditions and resource use efficiencies will be essential. Such differentiated policies are necessary to ensure that emission-reduction efforts are both effective and aligned with national sustainability objectives. The analysis of the relationship between per capita GDP and agricultural N_2O emissions in China aligns with an inverted "N"-shaped EKC, suggesting that emissions have generally entered a declining phase. However, Northeast and South China continue to face substantial emission-reduction pressures, emphasizing the necessity of tailored, region-specific mitigation policies rather than a "one-size-fits-all" strategy. Future research should explore broader socio-economic and environmental determinants of agricultural N_2O emissions and assess the sustained impacts of policy interventions across regional and national scales to refine emission reduction strategies.

Author Contributions: Conceptualization, M.B. and W.X.; Methodology, M.B. and G.W.; Formal analysis, Y.W.; Investigation, M.B.; Resources, G.W.; Data curation, G.W.; Writing—original draft, M.B.; Writing—review & editing, W.X.; Supervision, G.W.; Project administration, G.W.; Funding acquisition, G.W. All authors have read and agreed to the published version of the manuscript.

Funding: This research was funded by the Innovation Centre for Digital Business and Capital Development of Beijing Technology and Business University, grant number SZSK2022010, SZSK202206; The Ministry of education of Humanities and Social Science project, grant number 24YJA630084 and Shanxi Federation of Social Sciences, grant number SSKLZDKT2024085.

Institutional Review Board Statement: Not applicable.

Data Availability Statement: Data are available upon request.

Acknowledgments: The authors are also thankful to the anonymous reviewers and editor for their constructive feedback, which significantly improved the manuscript.

Conflicts of Interest: The authors declare no conflicts of interest.

References

1. Sanford, M.; Painter, J.; Yasseri, T.; Lorimer, J. Controversy around climate change reports: A case study of Twitter responses to the 2019 IPCC report on land. *Clim. Change* **2021**, *167*, 59. [CrossRef] [PubMed]
2. Kelley, L.A.; Zhang, Z.; Tamagno, S.; Lundy, M.E.; Mitchell, J.P.; Gaudin, A.C.; Pittelkow, C.M. Changes in soil N_2O emissions and nitrogen use efficiency following long-term soil carbon storage: Evidence from a mesocosm experiment. *Agric. Ecosyst. Environ.* **2024**, *370*, 109054. [CrossRef]
3. Xing, Y.; Wang, X. Impact of Agricultural Activities on Climate Change: A Review of Greenhouse Gas Emission Patterns in Field Crop Systems. *Plants* **2024**, *13*, 2285. [CrossRef] [PubMed]
4. Kumar, R.; Bordoloi, N. Combined impact of reduced N fertilizer and green manure on wheat yield, nitrogen use efficiency and nitrous oxide (N_2O) emissions reduction in Jharkhand, eastern India. *Field Crops Res.* **2024**, *318*, 109591. [CrossRef]

5. Müller, R. The impact of the rise in atmospheric nitrous oxide on stratospheric ozone: This article belongs to Ambio's 50th Anniversary Collection. Theme: Ozone Layer. *Ambio* **2021**, *50*, 35–39. [CrossRef]
6. Thompson, R.L.; Lassaletta, L.; Patra, P.K.; Wilson, C.; Wells, K.C.; Gressent, A.; Koffi, E.N.; Chipperfield, M.P.; Winiwarter, W.; Davidson, E.A. Acceleration of global N_2O emissions seen from two decades of atmospheric inversion. *Nat. Clim. Change* **2019**, *9*, 993–998. [CrossRef]
7. Lee, H.; Calvin, K.; Dasgupta, D.; Krinner, G.; Mukherji, A.; Thorne, P.; Trisos, C.; Romero, J.; Aldunce, P.; Barret, K. *IPCC, 2023: Climate Change 2023: Synthesis Report, Summary for Policymakers*; Contribution of Working Groups I, II and III to the Sixth Assessment Report of the Intergovernmental Panel on Climate Change; Core Writing Team, Lee, H., Romero, J., Eds.; IPCC: Geneva, Switzerland, 2023.
8. Menegat, S.; Ledo, A.; Tirado, R. Greenhouse gas emissions from global production and use of nitrogen synthetic fertilisers in agriculture. *Sci. Rep.* **2022**, *12*, 14490. [CrossRef]
9. Tian, H.; Yang, J.; Xu, R.; Lu, C.; Canadell, J.G.; Davidson, E.A.; Jackson, R.B.; Arneth, A.; Chang, J.; Ciais, P. Global soil nitrous oxide emissions since the preindustrial era estimated by an ensemble of terrestrial biosphere models: Magnitude, attribution, and uncertainty. *Glob. Change Biol.* **2019**, *25*, 640–659. [CrossRef] [PubMed]
10. Liang, M.; Zhou, Z.; Ren, P.; Xiao, H.; Hu, Z.; Piao, S.; Tian, H.; Tong, Q.; Zhou, F.; Wei, J. Four decades of full-scale nitrous oxide emission inventory in China. *Natl. Sci. Rev.* **2024**, *11*, nwad285. [CrossRef]
11. Harmsen, J.; van Vuuren, D.P.; Nayak, D.R.; Hof, A.F.; Höglund-Isaksson, L.; Lucas, P.L.; Nielsen, J.B.; Smith, P.; Stehfest, E. Long-term marginal abatement cost curves of non-CO_2 greenhouse gases. *Environ. Sci. Policy* **2019**, *99*, 136–149. [CrossRef]
12. Lynch, J.; Cain, M.; Frame, D.; Pierrehumbert, R. Agriculture's contribution to climate change and role in mitigation is distinct from predominantly fossil CO_2-emitting sectors. *Front. Sustain. Food Syst.* **2021**, *4*, 518039. [CrossRef] [PubMed]
13. Luo, Z.; Lam, S.K.; Fu, H.; Hu, S.; Chen, D. Temporal and spatial evolution of nitrous oxide emissions in China: Assessment, strategy and recommendation. *J. Clean. Prod.* **2019**, *223*, 360–367. [CrossRef]
14. Meyer-Aurich, A.; Karatay, Y.N. Greenhouse gas mitigation costs of reduced nitrogen fertilizer. *Agriculture* **2022**, *12*, 1438. [CrossRef]
15. Kakraliya, S.K.; Jat, H.S.; Sapkota, T.B.; Singh, I.; Kakraliya, M.; Gora, M.K.; Sharma, P.C.; Jat, M.L. Effect of climate-smart agriculture practices on climate change adaptation, greenhouse gas mitigation and economic efficiency of rice-wheat system in India. *Agriculture* **2021**, *11*, 1269. [CrossRef]
16. Laing, A.M.; Eckard, R.J.; Smith, A.P.; Grace, P. Twenty years of nitrous oxide emissions research in Australian agriculture: A review. *Agric. Ecosyst. Environ.* **2023**, *356*, 108638. [CrossRef]
17. Liu, C.M.; Sandhu, N.K.; McCoy, S.T.; Bergerson, J.A. A life cycle assessment of greenhouse gas emissions from direct air capture and Fischer–Tropsch fuel production. *Sustain. Energy Fuels* **2020**, *4*, 3129–3142. [CrossRef]
18. Ning, J.; Zhang, C.; Hu, M.; Sun, T. Accounting for Greenhouse Gas Emissions in the Agricultural System of China Based on the Life Cycle Assessment Method. *Sustainability* **2024**, *16*, 2594. [CrossRef]
19. Grados, D.; Butterbach-Bahl, K.; Chen, J.; van Groenigen, K.J.; Olesen, J.E.; van Groenigen, J.W.; Abalos, D. Synthesizing the evidence of nitrous oxide mitigation practices in agroecosystems. *Environ. Res. Lett.* **2022**, *17*, 114024. [CrossRef]
20. You, L.; Ros, G.H.; Chen, Y.; Yang, X.; Cui, Z.; Liu, X.; Jiang, R.; Zhang, F.; de Vries, W. Global meta-analysis of terrestrial nitrous oxide emissions and associated functional genes under nitrogen addition. *Soil Biol. Biochem.* **2022**, *165*, 108523. [CrossRef]
21. Fabregat-Aibar, L.; Niñerola, A.; Pié, L. Computable general equilibrium models for sustainable development: Past and future. *Environ. Sci. Pollut. Res.* **2022**, *29*, 38972–38984. [CrossRef]
22. Zhang, X.; Wu, L.; Ma, X.; Qin, Y. Dynamic computable general equilibrium simulation of agricultural greenhouse gas emissions in China. *J. Clean. Prod.* **2022**, *345*, 131122. [CrossRef]
23. Hu, B.; Zhang, L.; Liang, C.; Yang, X.; Shi, Z.; Wang, C. Characterizing Spatial and Temporal Variations in N_2O Emissions from Dairy Manure Management in China Based on IPCC Methodology. *Agriculture* **2024**, *14*, 753. [CrossRef]
24. Li, Z.; Fu, W.; Luo, M.; Chen, J.; Li, L. Calculation and scenario prediction of methane emissions from agricultural activities in China under the background of "carbon peak". *IOP Conf. Ser. Earth Environ. Sci.* **2022**, *1087*, 012021. [CrossRef]
25. Frank, S.; Havlík, P.; Stehfest, E.; van Meijl, H.; Witzke, P.; Pérez-Domínguez, I.; van Dijk, M.; Doelman, J.C.; Fellmann, T.; Koopman, J.F. Agricultural non-CO_2 emission reduction potential in the context of the 1.5 °C target. *Nat. Clim. Change* **2019**, *9*, 66–72. [CrossRef]
26. Rogelj, J.; Lamboll, R.D. Substantial reductions in non-CO_2 greenhouse gas emissions reductions implied by IPCC estimates of the remaining carbon budget. *Commun. Earth Environ.* **2024**, *5*, 35. [CrossRef]
27. Ou, Y.; Roney, C.; Alsalam, J.; Calvin, K.; Creason, J.; Edmonds, J.; Fawcett, A.A.; Kyle, P.; Narayan, K.; O'Rourke, P. Deep mitigation of CO_2 and non-CO_2 greenhouse gases toward 1.5 °C and 2 °C futures. *Nat. Commun.* **2021**, *12*, 6245. [CrossRef]
28. Lin, J.; Khanna, N.; Liu, X.; Wang, W.; Gordon, J.; Dai, F. Opportunities to tackle short-lived climate pollutants and other greenhouse gases for China. *Sci. Total Environ.* **2022**, *842*, 156842. [CrossRef]
29. Huang, T.; Yang, H.; Huang, C.; Ju, X. Effects of nitrogen management and straw return on soil organic carbon sequestration and aggregate-associated carbon. *Eur. J. Soil Sci.* **2018**, *69*, 913–923. [CrossRef]
30. Searchinger, T.D.; Wirsenius, S.; Beringer, T.; Dumas, P. Assessing the efficiency of changes in land use for mitigating climate change. *Nature* **2018**, *564*, 249–253. [CrossRef]

31. Gavrilova, O.; Leip, A.; Dong, H.; MacDonald, J.; Bravo, C.; Amon, B.; Rosales, R.; Prado, A.; Lima, M.; Oyhantçabal, W. Proceedings of the IPCC 2019 Refinement of IPCC 2006 Guidelines for National Greenhouse Gas Inventories; Geneva, Switzerland, 2019; pp. 1–207. Available online: https://www.ipcc-nggip.iges.or.jp/public/2019rf/pdf/4_Volume4/19R_V4_Ch10_Livestock.pdf (accessed on 11 November 2024).
32. National Development and Reform Commission. Guidelines for the Preparation of Provincial Greenhouse Gasinventories (Trial). Available online: http://www.cbcsd.org.cn/sjk/nengyuan/standard/home/20140113/download/shengjiwenshiqiti.pdf (accessed on 11 October 2024).
33. Yu, Z.; Zhang, F.; Gao, C.; Mangi, E.; Ali, C. The potential for bioenergy generated on marginal land to offset agricultural greenhouse gas emissions in China. *Renew. Sustain. Energy Rev.* **2024**, *189*, 113924. [CrossRef]
34. Wang, Y.; Zhu, Y.; Zhang, S.; Wang, Y. What could promote farmers to replace chemical fertilizers with organic fertilizers? *J. Clean. Prod.* **2018**, *199*, 882–890. [CrossRef]
35. Gao, F.; Lv, K.; Qiao, Z.; Ma, F.; Jiang, O. Assessment and prediction of carbon neutrality in the eastern margin ecotone of Qinghai-Tibet Plateau. *Sheng Tai Xue Bao* **2022**, *42*, 9442–9455. [CrossRef]
36. Zhao, L.; Zhao, T.; Yuan, R. Scenario simulations for the peak of provincial household CO_2 emissions in China based on the STIRPAT model. *Sci. Total Environ.* **2022**, *809*, 151098. [CrossRef]
37. Ministry of Agriculture and Rural Affairs. Ministry of Agriculture and Rural Affairs Issued the "14th Five-Year Plan" National Agricultural Mechanization Development Plan. 5 January 2022. Available online: http://www.moa.gov.cn/xw/zwdt/202201/t20220105_6386352.htm (accessed on 11 October 2024).
38. Jiang, J.; Zhao, T.; Wang, J. Decoupling analysis and scenario prediction of agricultural CO_2 emissions: An empirical analysis of 30 provinces in China. *J. Clean. Prod.* **2021**, *320*, 128798. [CrossRef]
39. Wang, Y.; Yuan, Y.; Yuan, F.; Ata-UI-Karim, S.T.; Liu, X.; Tian, Y.; Zhu, Y.; Cao, W.; Cao, Q. Evaluation of Variable Application Rate of Fertilizers Based on Site-Specific Management Zones for Winter Wheat in Small-Scale Farming. *Agronomy* **2023**, *13*, 2812. [CrossRef]
40. Popa, D.C.; Laurent, Y.; Popa, R.A.; Pasat, A.; Bălănescu, M.; Svertoka, E.; Pogurschi, E.N.; Vidu, L.; Marin, M.P. A Platform for GHG Emissions Management in Mixed Farms. *Agriculture* **2023**, *14*, 78. [CrossRef]
41. Nisbet, E.G.; Dlugokencky, E.J.; Fisher, R.E.; France, J.L.; Lowry, D.; Manning, M.R.; Michel, S.E.; Warwick, N.J. Atmospheric methane and nitrous oxide: Challenges alongthe path to Net Zero. *Philos. Trans. R. Soc. A* **2021**, *379*, 20200457. [CrossRef]
42. Kuang, W.; Gao, X.; Tenuta, M.; Zeng, F. A global meta-analysis of nitrous oxide emission from drip-irrigated cropping system. *Glob. Change Biol.* **2021**, *27*, 3244–3256. [CrossRef] [PubMed]
43. Hamad, A.A.A.; Wei, Q.; Wan, L.; Xu, J.; Hamoud, Y.A.; Li, Y.; Shaghaleh, H. Subsurface drip irrigation with emitters placed at suitable depth can mitigate N2O emissions and enhance Chinese cabbage yield under greenhouse cultivation. *Agronomy* **2022**, *12*, 745. [CrossRef]
44. Shi, R.; Irfan, M.; Liu, G.; Yang, X.; Su, X. Analysis of the impact of livestock structure on carbon emissions of animal husbandry: A sustainable way to improving public health and green environment. *Front. Public Health* **2022**, *10*, 835210. [CrossRef]
45. Puertas, R.; Marti, L.; Calafat, C. Agricultural and innovation policies aimed at mitigating climate change. *Environ. Sci. Pollut. Res.* **2023**, *30*, 47299–47310. [CrossRef] [PubMed]
46. Jiang, H.-D.; Yu, R.; Qian, X.-Y. Socio-economic and energy-environmental impacts of technological change on China's agricultural development under the carbon neutrality strategy. *Pet. Sci.* **2023**, *20*, 1289–1299. [CrossRef]
47. Liu, M.; Yang, L. Spatial pattern of China's agricultural carbon emission performance. *Ecol. Indic.* **2021**, *133*, 108345. [CrossRef]